Self-Assembly of Ball-Shaped Molecular Complexes in Water

Thomas Grawe,[†] Thomas Schrader,*[,‡] Reza Zadmard,[‡] and Arno Kraft*[,§]

Institut für Organische Chemie und Makromolekulare Chemie, Heinrich-Heine-Universität Düsseldorf, Universitätsstr. 1, D-40225 Düsseldorf, Germany, Fachbereich Chemie, Philipps-Universität Marburg, Hans-Meerwein-Str., D-35032 Marburg, Germany, and Department of Chemistry, Heriot-Watt University, Riccarton, Edinburgh EH14 4AS, United Kingdom

schradet@mailer.uni-marburg.de

Received January 9, 2002

We present a simple and versatile access to spheroidal molecular assemblies with pronounced stability in highly polar solvents. These complexes are composed of doubly and triply charged complementary building blocks based on ammonium or amidinium cations and phosphonate anions. Their high thermodynamic stability is best explained by the formation of a cyclic array of alternating positive and negative charges interconnected by a regular network of hydrogen bonds. Association constants reach 10^6 M^{-1} in methanol and often surpass 10^3 M^{-1} in water. The broad range of binding energies correlates well with the varying degree of preorganization of both complex partners. As a byproduct of these investigations, new recognition motifs for histidine and arginine esters and the unsubstituted guanidinium ion are proposed. The additional introduction of methyl groups in the 2-, 4-, and 6-positions of the central benzene ring in either cations or anions causes a marked drop in the corresponding K_a values of 1 order of magnitude; the related rotational barriers were estimated at 0.3−2.1 kcal/mol. Spontaneous formation of defined 2:1 complexes from three components has also been observed.

Introduction

Self-organized molecular containers have been extensively used by Nature in various forms. Proteasomes, which are able to digest almost any protein molecule, are well-defined barrel-shaped molecular assemblies that form spontaneously from up to 40 components.[1] Viruses are another case of helical or spherical container superstructures with a self-assembled protein coat that protects the viral nucleic acids.[2] These natural examples inspired many supramolecular chemists to design molecular building blocks that are able to self-assemble into larger capsule-like ensembles. The simplest access to self-organized capsules is the well-known preparation of vesicles from phospholipids. During the past decade, emulsion and interface polymerization have both been used to construct various types of concave and porous polymeric analogues.[3] Recent advances include the self-organization of amphiphilic block copolymers with subsequent cross-linking of their coat and destruction of the nucleus inside.[4] The geometrically well-defined coordination sphere of transition metal cations has also been explored for the programmed design of multicomponent aggregates, in some cases reminiscent of the viroidal coat.[5] Other approaches made extensive use of hydrophobic interactions as, for example, cyclodextrin dimers.[6] Particularly in nonpolar solvents, self-complementary building blocks capable of forming multiple hydrogen bonds with each other will self-assemble into closed architectures.[7] These molecular capsules can accommodate guest molecules of the right size and polarity. A

[†] University of Düsseldorf.

[‡] University of Marburg. Phone: +49-6421-2825544.

[§] Heriot-Watt University.

(1) (a) Voges, D.; Zwickl, P.; Baumeister, W. *Annu. Rev. Biochem.* **1999**, *68*, 1015−1068. (b) Kruger, E.; Kloetzel, P. M.; Enenkel, C. *Biochimie* **2001**, *83*, 289−293.

(2) Klug, A. *Angew. Chem., Int. Ed. Engl.* **1983**, *22*, 565−582.

(3) (a) Overview: Donath, E.; Sukhorukov, G. B.; Möhwald, H. *Nachr. Chem. Technol. Lab.* **1999**, *47*, 400−404 and refs cited therein. (b) Kong, X. Z.; Kan, C. Y.; Li, H. H.; Yu, D. Q.; Yuan, Q. *Polym. Adv. Technol.* **1997**, *8*, 627−630.

(4) (a) Thurmond, K. B.; Kowalewski, T.; Wooley, K. L. *J. Am. Chem. Soc.* **1997**, *119*, 6656−6665. (b) Donath, E.; Sukhorukov, G. B.; Caruso, F.; Davies, S. A.; Möhwald, H. *Angew. Chem., Int. Ed.* **1998**, *37*, 2202−2205.

(5) Metal chelates: (a) Lehn, J. M. *Angew. Chem., Int. Ed. Engl.* **1990**, *29*, 1304−1319. (b) Lee, J.; Schwabacher, A. W. *J. Am. Chem. Soc.* **1994**, *116*, 8382−8383. (c) Klüfers, P.; Schuhmacher, J. *Angew. Chem., Int. Ed. Engl.* **1994**, *33*, 1863−1865. (d) Saalfrank, R. W.; Burak, R.; Reihs, S.; Löw, N.; Hampel, F.; Stachel, H.-D.; Lentmaier, J.; Peters, K.; Peters, E. M.; von Schnering, H. G. *Angew. Chem., Int. Ed. Engl.* **1995**, *34*, 993−995. (e) Takeda, N.; Umemoto, K.; Yamaguchi, K.; Fujita, M. *Nature* **1999**, *398*, 794−796. (f) Olenyuk, B.; Whiteford, J. A.; Fechtenkötter, A.; Stang, P. J. *Nature* **1999**, *398*, 796−798. (g) Olenyuk, B.; Levin, M. D.; Whiteford, J. A.; Shield, J. E.; Stang, P. J. *J. Am. Chem. Soc.* **1999**, *121*, 10434−10435. (h) Leininger, S.; Olenyuk, B.; Stang, P. J. *Chem. Rev.* **2000**, *100*, 853−908. (i) Umemoto, K.; Yamaguchi, K.; Fujita, M. *J. Am. Chem. Soc.* **2000**, *122*, 7150−7151. (j) Fujita, N.; Biradha, K.; Fujita, M.; Sakamoto, S.; Yamaguchi, K. *Angew. Chem., Int. Ed.* **2001**, *40*, 1718−1721.

(6) Hydrophobic capsules: (a) Harada, A.; Takahashi, S. *J. Chem. Soc., Chem. Commun.* **1988**, 1352−1353. (b) Boulas, P.; Kutner, W.; Jones, M. T.; Kadish, K. M. *J. Phys. Chem.* **1994**, *98*, 1282−1287. (c) Zhao, S.; Luong, J. H. T. *J. Chem. Soc., Chem. Commun.* **1995**, 663−664. (d) Venema, F.; Rowan, A. E.; Nolte, R. J. M. *J. Am. Chem. Soc.* **1996**, *118*, 257−258.

(7) (a) For an excellent review, see: Conn, M. M.; Rebek, J. *Chem. Rev.* **1997**, *97*, 1647−1668. Some more recent work on self-organized molecular capsules based on hydrogen bonds: (b) Kikuchi, Y.; Tanaka, Y.; Sutarto, S.; Kobayashi, K.; Toi, H.; Aoyama, Y. *J. Am. Chem. Soc.* **1992**, *114*, 10302−10306. (c) Mammen, M.; Simanek, E. E.; Whitesides, G. M. *J. Am. Chem. Soc.* **1996**, *118*, 12614−12623. (d) Vreekamp, R. H.; Verboom, W.; Reinhoudt, D. N. *J. Org. Chem.* **1996**, *61*, 4282−4288. (e) Mogck, O.; Böhmer, V.; Vogt, W. *Tetrahedron* **1996**, *52*, 8489−8496. (f) Sessler, J. L.; Wang, R. *J. Am. Chem. Soc.* **1996**, *118*, 9808−9809. (g) Heinz, T.; Rudkevich, D. M.; Rebek, J. *Nature* **1998**, *394*, 764−767. (h) Martín, T.; Obst, U.; Rebek, J. *Science* **1998**, *281*, 1842−1845. (i) Prins, L. J.; Huskens, J.; de Jong, F.; Timmerman, P.; Reinhoudt, D. N. *Nature* **1999**, *398*, 498−502. (j) Hof, F.; Nuckolls, C.; Craig, S. L.; Martín, T.; Rebek, J. *J. Am. Chem. Soc.* **2000**, *122*, 10991−10996. (k) Rivera, J. M.; Craig, S. L.; Martín, T.; Rebek, J. *Angew. Chem., Int. Ed.* **2000**, *39*, 2130−2132.

10.1021/jo025513y CCC: $22.00
Published on Web 05/09/2002

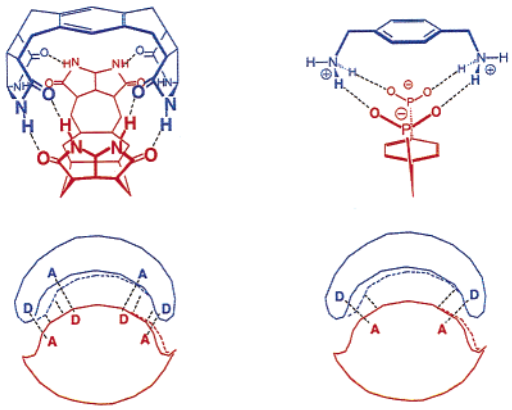

Figure 1. Comparison between a well-known self-organizing molecular assembly composed of self-complementary building blocks (e.g., Rebek's tennisball)[8] and our simple system based on complementary moieties. D/A = Hydrogen bond donor/acceptor. Note that the system on the left is held together merely by hydrogen bonds, whereas the system on the right makes use of ion-pair-reinforced hydrogen bonds that provide additional stability in polar organic media such as DMSO and methanol.

prominent example is the supramolecular tennisball created by Rebek and co-workers.[8] However, most of these model systems rely on weak, albeit directed, hydrogen bonds, and they are hence restricted exclusively to nonpolar solvents.[9] We found recently that spheroidal molecular assemblies in polar organic media can be achieved with high stability provided that multiple electrostatic interactions are generated between two complementary building blocks.[10] An alternating array of positive and negative charges leads to multiple chelate arrangements, assisted by strong ionic hydrogen bonds. This design principle was originally recognized with complexes between dications and dianions and later successfully transferred to trication−trianion combinations.

Results and Discussion

Complexes between Bisphosphonates and Organic α,ω-Dications. At the outset of our investigation, we noted that certain α,ω-bisphosphonates are attracted by α,ω-diammonium cations. Molecular dynamics calculations reproducibly lead to highly symmetrical cyclic arrangements with alternating negative and positive charges interconnected by a network of hydrogen bonds. These simple three-dimensional structures bear a certain resemblance to Rebek's tennisball (Figure 1). In both cases, complementary building blocks are attracted toward each other through hydrogen bonds, thereby resulting in spheroidal structures of similar overall symmetry. However, bisphosphonates and diammonium moieties are ionic species, and they are therefore expected to give strong complexes even in highly polar organic media. In this respect, the above-mentioned ionic assemblies also

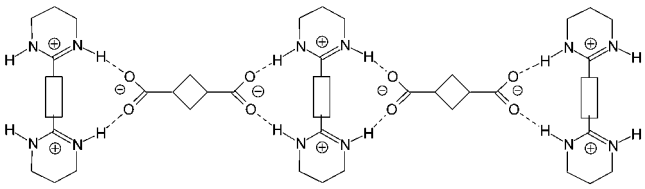

Figure 2. Hosseini's supramolecular networks from dicarboxylates and bridging bisamidinium derivatives.[11]

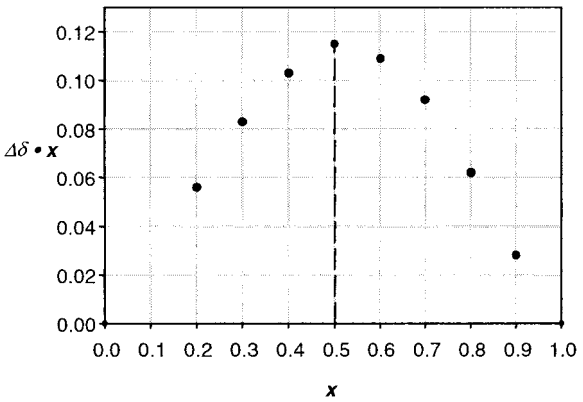

Figure 3. Job plot for the complex between bisphosphonate **1** and histidine methyl ester **6**. The mole fraction *x* of **1** is defined as [**1**]/([**1**] + [**6**]). The total concentration was maintained at 2.3 mM, and the change in chemical shift of the receptor's methyl ester signal was determined for various compositions.

parallel the two-dimensional supramolecular networks that Hosseini et al. obtained with combinations of planar bisamidinium salts and dicarboxylates in a "crystal engineering" approach (Figure 2).[11]

During preliminary investigations, we simply mixed equimolar solutions of xylylene bisphosphonates[12] and the respective diammonium salts. The first hint of strong binding came from the observation that the 1:1 complexes derived from the *p*-xylylene derivatives precipitated quantitatively from DMSO in an analytically pure form, whereas the *m*-xylylene derivatives instead gave soluble species with sharp signals in the ^{1}H, ^{13}C, and ^{31}P NMR spectra. The formation of nonpolymeric complexes with a 1:1 stoichiometry was evident from a Job plot (Figure 3).[13] The complex geometry postulated in Figure 4 is further supported by strong upfield shifts (up to 0.8 ppm) for all bridging diammonium alkyl groups as they experience the deshielding effect above the host's benzene ring. Another indication comes from the strong downfield shift of the aromatic guest protons H-4 to H-6 in a complex between **1** and **3**. To avoid steric strain, the benzene ring of the guest is expected to lower down just above one of the host's phosphonate esters.

(8) Molecular tennisballs: (a) Wyler, R.; de Mendoza, J.; Rebek, J. *Angew. Chem., Int. Ed. Engl.* **1993**, *32*, 1699−1701. (b) Branda, N.; Wyler, R.; Rebek, J. *Science* **1994**, *263*, 1267−1268.

(9) Recent advances with hydrogen bonds in polar solvents: (a) Vysotsky, M. O.; Thondorf, I.; Böhmer, V. *Chem. Commun.* **2001**, 1890−1891. (b) Shivanyuk, A.; Rebek, J. *Chem. Commun.* **2001**, 2374−2375. (c) Atwood, J. L.; Barbour, L. J.; Jerga, A. *Chem. Commun.* **2001**, 2376−2377.

(10) (a) Grawe, T.; Schrader, T.; Gurrath, M.; Kraft, A.; Osterod, F. *Org. Lett.* **2000**, *2*, 29−32. (b) Grawe, T.; Schrader, T.; Gurrath, M.; Kraft, A.; Osterod, F. *J. Phys. Org. Chem.* **2000**, *13*, 670−673.

(11) (a) Hosseini, M. W.; Ruppert, R.; Schaeffer, P.; De Cian, A.; Kyritsakas, N.; Fischer, J. *J. Chem. Soc., Chem. Commun.* **1994**, 2135−2136. (b) Brand, G.; Hosseini, M. W.; Ruppert, R.; De Cian, A.; Fischer, J.; Kyritsakas, N. *New J. Chem.* **1995**, *19*, 9−13. (c) Hosseini, M. W.; Brand, G.; Schaeffer, P.; Ruppert, R.; De Cian, A.; Fischer, J. *Tetrahedron Lett.* **1996**, *37*, 1405−1408. (d) Félix, O.; Hosseini, M. W.; De Cian, A.; Fischer, J. *Angew. Chem., Int. Ed. Engl.* **1997**, *36*, 102−104. (e) Félix, O.; Hosseini, M. W.; De Cian, A.; Fischer, J. *Tetrahedron Lett.* **1997**, *38*, 1933−1936. (f) Russell, V. A.; Ward, M. D. *Chem. Mater.* **1996**, *8*, 1654−1666.

(12) Xylylene bisphosphonates were prepared according to published procedures: Schrader, T. *J. Org. Chem.* **1998**, *63*, 264−272.

(13) (a) Job, P. *Ann. Chim.* **1928**, *9*, 113−203. (b) Blanda, M. T.; Horner, J. H.; Newcomb, M. *J. Org. Chem.* **1989**, *54*, 4626−4636.

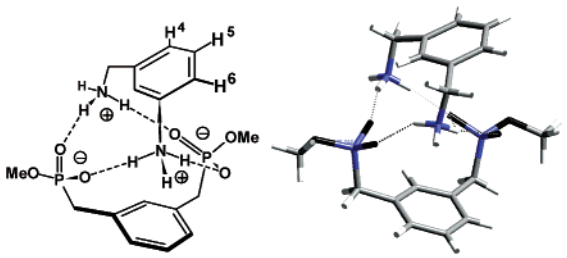

Figure 4. Energy-minimized structure of the complex between *m*-xylylene bisphosphonate **1** and *m*-xylylene diammonium salt **3**. Left: Lewis structure. Right: cylinder model (Cerius^2, MSI, Dreiding 2.21).

Table 1. Association Constants K_a for the 1:1 Complexes between α,ω-Diammonium Derivatives and 1 from NMR Titrations in DMSO-d_6 at 20 °C[a]

diamine hydrochloride	K_a [M^{-1}]
1,2-diaminocyclohexane (**2**)	1.4×10^3
m-xylylenediamine (**3**)	1.6×10^3
1,3-diaminopropane (**4**)	2.8×10^3
N-methyl-1,3-diaminopropane	3.2×10^3
lysine methyl ester (**5**)	5.0×10^3
histidine methyl ester (**6**)	8.0×10^3
arginine methyl ester (**7**)	1.6×10^3

[a] As a result of the strongly hygroscopic character of both titration partners, the DMSO-d_6 solutions contained ~0.1% of water. Errors in K_a are standard deviations from the nonlinear regression; they were calculated at $10\% \leq K_a \leq 50\%$.

We carried out NMR titrations of bisphosphonate **1** with a broad range of diammonium salts in DMSO-d_6 and calculated the association constants by nonlinear regression.[14] Table 1 shows that all association constants K_a lie between 10^3 and 10^4 M^{-1}, which incidentally is not much higher than the comparable association constants of **1** with simple monoamines.[15] Obviously, bond distances and angles in the bisphosphonate−bisammonium hydrogen bond network are far from ideal. This may stem from the fact that the second ammonium group has to push the first one out of its chelated arrangement between both phosphonates.[15] It is interesting to note that within this series, binding constants increase with increasing length of the alkyl chain between the cationic head and tail group (**2**−**5**). Although the bisphosphonate distance remains constant throughout the series, it may constitute another example of the beneficial effect of guest flexibility as opposed to loss of preorganization.[16]

The highest association constants are measured for two basic amino acids. Histidine ester **6** is particularly interesting because, during its NMR titration with **1**, both aromatic imidazolium-CH protons are shifted upfield by 1.1 and 1.2 ppm, respectively. The imidazolium ring is apparently located just above the host's aromatic ring and, thus, involved in efficient π-cation as well as π−π interactions.[17]

Complexes between Trisphosphonates and Organic Trications. Anslyn[18] und Lehn[19] have previously demonstrated that it is possible to achieve strong binding in water by an efficient combination of three or four ion pairs even in the absence of hydrophobic interactions. Trisphosphonate **8** is the logical extension of our above-described concept of alternating charges. The compound should be able to form a C_{3v}-symmetrical complex with a matching triammonium ligand. Molecular mechanics calculations again predict a highly symmetrical spheroidal complex geometry with almost linear hydrogen bonds (Figure 5).[20]

This array is calculated to be far more stable than the respective simple ion pairs.[22] A Michaelis−Arbuzow reaction between trimethyl phosphite and tris(bromomethyl)benzenes furnished trisphosphonates **8** and **9** in high yields (Scheme 1). The phosphonates were subsequently monodealkylated with tetrabutylammonium hydroxide.

The tricationic counterparts are displayed in Scheme 4. They were synthesized either as trisamidinium or as triammonium derivatives. Heterocyclic trisamidines **10** and **11** were prepared by a one-step route from benzene-1,3,5-tricarboxylic acid.[23] Trisamidine **12** was obtained in two steps from the corresponding ethyl amide.[24] Cyclohexanetriamine **13** was prepared from *cis*,*cis*-1,3,5-cyclohexanetricarboxylic acid by a Curtius rearrangement.[25] The mesitylene triamines **14** and **15** were accessible via the corresponding trisphthalimides and subsequent hydrazinolysis (Scheme 2).

Finally, tris(pyrazolyl)-substituted mesitylenes **16** and **17** were obtained from the same two 1,3,5-tris(bromomethyl)benzenes after triple nucleophilic substitution with pyrazole (Scheme 3).[26] C_3-Symmetrical trispyrazole compounds such as **16** and **17** in the form of the free base have recently been used as metal-encapsulating ligands[27] and as highly efficient ammonium receptors.[28] Crystal structures show that all pyrazole groups are oriented toward one side of the central benzene ring with the basic

(14) (a) Schneider, H.-J.; Kramer, R.; Simova, S.; Schneider, U. *J. Am. Chem. Soc.* **1988**, *110*, 6442−6448. (b) Wilcox, C. S. In *Frontiers in Supramolecular Chemistry and Photochemistry*; Schneider, H.-J., Dürr, H., Eds.; VCH: Weinheim, Germany, 1991; pp 123−143. (c) Macomber, R. S. *J. Chem. Educ.* **1992**, *69*, 375−378.

(15) (a) Schrader, T. *Angew. Chem., Int. Ed. Engl.* **1996**, *35*, 2649−2651. (b) Schrader, T. *J. Org. Chem.* **1998**, *63*, 264−272.

(16) Eblinger, F.; Schneider, H.-J. *Angew. Chem., Int. Ed.* **1998**, *37*, 826−829.

(17) A similar observation was made in macrocyclic tetraphosphonate hosts that bind histidine esters strongly in water: Grawe, T.; Schrader, T.; Finocchiaro, P.; Consiglio, G.; Failla, S. *Org. Lett.* **2001**, *3*, 1597−1600.

(18) Metzger, A.; Lynch, V. M.; Anslyn, E. V. *Angew. Chem., Int. Ed. Engl.* **1997**, *109*, 862−865.

(19) (a) Hosseini, M. W.; Lehn, J.-M.; Mertes, M. P. *Helv. Chim. Acta* **1983**, *66*, 2454−2466. (b) Hosseini, M. W.; Lehn, J.-M.; Maggiora, L.; Mertes, K. B.; Mertes, M. P. *J. Am. Chem. Soc.* **1987**, *109*, 537−544.

(20) (a) A relatively vague self-organization of a molecular capsule based on flexible ammonium carboxylate ion pairs has been described: Lee, S. B.; Hong, J.-I. *Tetrahedron Lett.* **1996**, *37*, 8501−8504. (b) Recently, a highly stable cage-like complex has been assembled from tetracationic Zn-porphyrinates and tetraanionic calixarenes: Fiammengo, R.; Timmerman, P.; de Jong, F.; Reinhoudt, D. N. *Chem. Commun.* **2000**, 2313−2314.

(21) (a) Connolly, M. L. *Science* **1983**, *221*, 709−713. (b) Connolly, M. L. *J. Appl. Crystallogr.* **1983**, *16*, 548.

(22) For flat structures, which form simple ion pairs, see: Schneider, H.-J.; Schiestel, T.; Zimmermann, P. *J. Am. Chem. Soc.* **1992**, *114*, 7698−7703.

(23) (a) Kraft, A.; Fröhlich, R. *Chem. Commun.* **1998**, 1085−1086. (b) Kraft, A.; Osterod, F. *J. Chem. Soc., Perkin Trans. 1* **1998**, 1019−1025. (c) Kraft, A.; Reichert, A. *Tetrahedron* **1999**, *55*, 3923−3930.

(24) (a) Kraft, A. *J. Chem. Soc., Perkin Trans. 1* **1999**, 705−714. Three crystal structures of an *N*,*N*′-diethyl-substituted benzamidine and its complexes confirm the almost perpendicular torsion angle between the amidine moiety and an adjacent benzene ring: (b) Peters, L.; Fröhlich, R.; Boyd, A. S. F.; Kraft, A. *J. Org. Chem.* **2001**, *66*, 3291−3298.

(25) Bowen, T.; Planalp, R. P.; Brechbiel, M. W. *Bioorg. Med. Chem. Lett.* **1996**, *6*, 807−810.

(26) Hartshorn, C. M.; Steel, P. J. *Aust. J. Chem.* **1995**, *48*, 1587−1599.

(27) Hartshorn, C. M.; Steel, P. J. *Angew. Chem., Int. Ed. Engl.* **1996**, *35*, 2655−2657.

(28) Chin, J.; Walsdorff, C.; Stranix, B.; Oh, J.; Chung, H. J.; Park, S.-M.; Kim, K. *Angew. Chem., Int. Ed.* **1999**, *38*, 2756−2759.

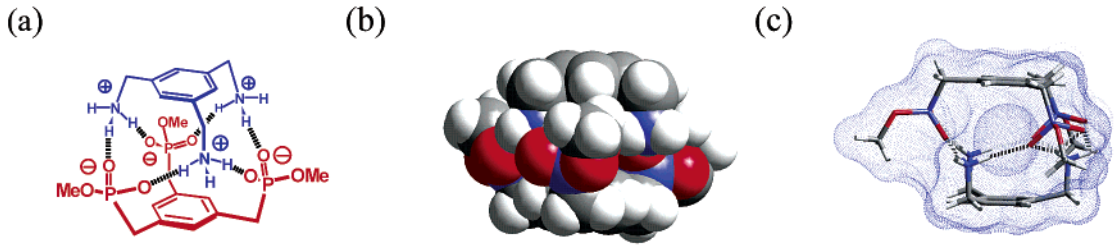

Figure 5. Energy-minimized structure of the complex between 1,3,5-trisphosphonate **8** and its analogous triammonium salt: (a) Lewis structure; (b) front view of the corresponding CPK model; (c) calculated van der Waals surface shown as Connolly surface[21] (dotted solvent-accessible area around the complex) with an internal cavity.

Scheme 1. Synthesis of Trisphosphonate Building Blocks

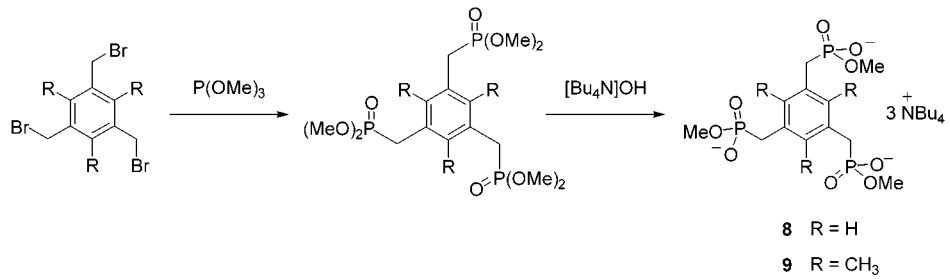

8 R = H
9 R = CH_3

Scheme 2. Synthesis of Mesitylene Triammonium Building Blocks

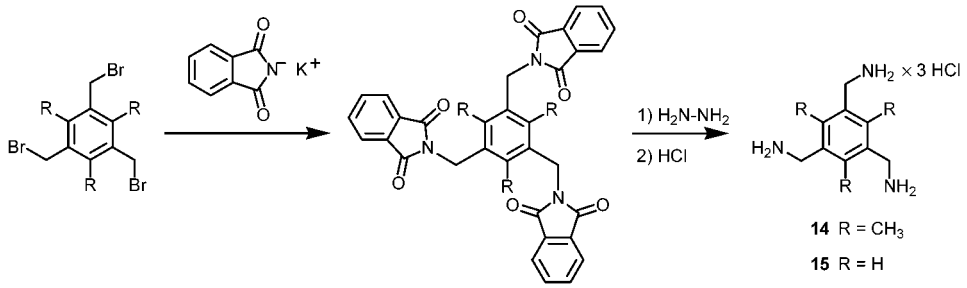

14 R = CH_3
15 R = H

Scheme 3. Synthesis of Trispyrazolylbenzene Building Blocks

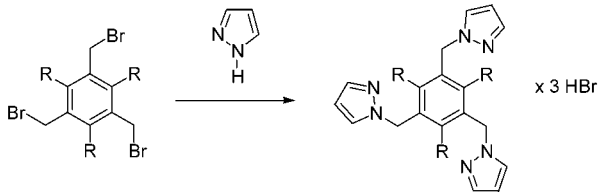

16 R = CH_3
17 R = H

nitrogen atoms pointing into the interior of the molecule.[26,27]

The high number of possible half-spheres resulting in assemblies of varying size and geometry demonstrates a substantial gain in flexibility as opposed to the self-complementary "one subunit−one complex" strategy. All the complexes prepared from **8** and various tricationic components produced sharp NMR signals as well as perfect 1:1 stoichiometries.[29] Chemical ionization mass spectrometry produced a weak molecular ion peak for the 1:1 complex of **8** and trisamidine **12** (1% for the M + NH_4^+ ion at m/z = 792), and no additional peaks were observed for higher aggregates. Electrospray ionization (ESI) mass spectrometry is a much milder technique, which proved to be advantageous for detecting the molecular ion peak of the same complex between **8** and **12**. An ESI mass spectrum could be obtained from a 10^{-7} M solution in methanol. The molecular ion peak M + H^+ (7% at m/z = 775) was found in the positive mass range, whereas in the negative mass range an M^- ion peak (5% at m/z = 774) was observed. Apparently, the capsule can pick up a proton with its anionic building block or lose a proton from its cationic moiety without falling apart. We note that ESI-MS could be a promising analytical tool for identifying changes in either half-sphere of the ionic capsules. This may, at a later stage, be of great value for detecting capsules with included neutral or charged guest molecules.

Chemically induced upfield shifts for *CH*-protons in some cases surpassed 0.5 ppm in DMSO-d_6, pointing to strong interactions. The results of selected NMR titrations with association constants K_a in DMSO-d_6 are shown in Table 2. All these entries indicate a slightly increased affinity of the complementary counterparts compared to our previously discussed dication−dianion

(29) In principle, 2:2 or 3:3 complexes could also be formed. However, at high contrentations, we observed another interesting effect, namely, extreme line-broadening of both NMR signals of the phosphonate esters in the trisphosphonate half-sphere **8** in its complex with trisamidine **12**. This must be a concentration-dependent dynamic effect: contrary to the preorganized amidinium groups, the phosphonate esters have to be frozen in their rotation around their benzylic and ester bonds, if a the proposed 1:1-complex geometry is reached, with an alternating array of arms coming from the top and bottom parts. Thus, the selective line-broadening of these two phosphonate signals constitutes a good indicator for formation of the 1:1-complex.

Scheme 4 C_{3v}**-Symmetrical Triammonium/Trisamidinium Cations and Hexaza-18-crown-6 (19) Used for NMR Titrations with Trisphosphonate 1**[a]

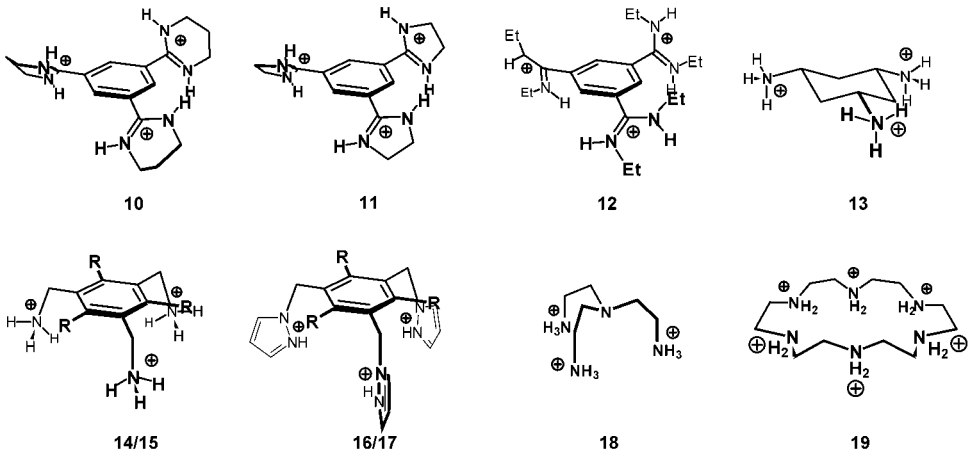

[a] All structures are depicted in the conformation necessary for complexation.

Table 2. Association Constants K_a for the 1:1 Complexes between Selected Trications and Trisphosphonate 8 from NMR Titrations in DMSO-d_6 at 20 °C[a]

trisamidine hydrochloride	K_a [M^{-1}]	other C_3-symmetrical cations	K_a [M^{-1}]
trisimidazoline **10**	9.5×10^3	guanidinium	3.6×10^4
tris(tetrahydropyrimidine) **11**	2.1×10^4	1,4,7-triazacyclononane	(2:1)[b]

[a] As a result of the strongly hygroscopic character of both titration partners, the DMSO-d_6 solution contained ~0.1% water. Errors in K_a are standard deviations from the nonlinear regression; they were calculated at 10% ≤ K_a ≤ 50%. [b] Strongly sigmoidal binding curve could not be fitted with conventional 2:1 equations; a highly cooperative binding is assumed.

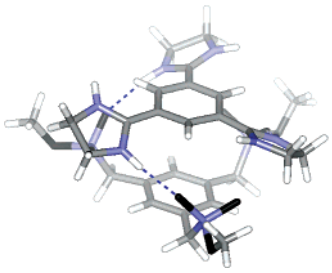

Figure 6. Proposed complex geometry between trisimidazoline **10** and trisphosphonate **8** according to molecular mechanics calculations.

complexes, albeit the difference is not very pronounced. Modeling experiments reveal that the two cyclic amidines **10** and **11** have to rotate the amidinium moieties out of the plane of the central benzene ring prior to binding to the trisphosphonate (Figure 6). The result is a substantial loss of delocalization energy reflected in the moderate binding constants. In addition, a notable upfield shift of the aromatic sensor proton[30] was observed as, obviously, the twisted amidinium substituents in the complex no longer withdraw electron density from the adjacent benzene ring.[31]

The guanidinium cation is C_3-symmetrical, too. Although it carries only a single positive charge, its binding constant clearly surpasses that of trications **10** and **11**. We attribute this to additional π-cationic interactions that become effective once the guanidinium moiety is located directly on top of the central phenyl ring at a calculated, almost ideal, distance of 3.2 Å. With the smallest possible azacrown (1,4,7-triazacyclononane), a strongly sigmoidal binding curve is obtained, which just about reaches its saturation point after addition of a second equiv of trisphosphonate **8**. A 2:1 complex is formed, as confirmed by a Job plot, with a high degree of cooperativity. We assume that the initial binding of a trisphosphonate preorients the azacrown, which then facilitates the docking of a second molecule of **8**.

With more flexible or better preorganized guest molecules, however, binding energies rise sharply and become too high in DMSO to be determined accurately by NMR techniques. We turned therefore to the more polar solvent methanol, which normally reduces association constants for purely electrostatic interactions by a factor of about 100. As Table 3 demonstrates, K_a values in methanol reach from 10^3 to 10^6 M^{-1} in the most favorable cases. Hence, they are up to 5 orders of magnitude larger than those obtained with their C_{2v}-symmetrical analogues (Scheme 4, Table 3).

We did not observe any chemically induced shifts for the ^{1}H NMR signals of the tetrabutylammonium counterions. Nevertheless, counterions could still play an important role in the early phase of the binding process. It is conceivable, for example, that even before complexation the chloride counterions of the trisammonium moiety occupy those places that are later taken over by the phosphonate groups. Hence, they would build a network of alternating positive and negative charges with a certain degree of productive preorientation.

(30) Complexes of **10** and **11** with monocarboxylates show the contrary, namely, a distinct downfield shift of the aromatic sensor protons. This is explained by the overall flattened complex geometry and has been confirmed by crystal structures: Osterod, F.; Peters, L.; Kraft, A.; Sano, T.; Morrison, J. J.; Feeder, N.; Holmes, A. B. *J. Mater. Chem.* **2001**, *11*, 1625−1633. In these complexes, the bridging carboxylates come into close contact with the trisamidine's benzene protons, thus causing the above-mentioned downfield shift.

(31) The torsion angle from force-field calculations amounts to 27° (**11**) and 31° (**10**), bringing both central benzene rings in complex **8**·**10** closer to each other: the distance between both central benzene rings is ~4.33 Å in the complex with **11**, but only ~4.21 Å in a complex with **10**. This correlates well with the higher K_a value for the tetrahydropyrimidine. In both complexes, the hydrogen bonds are all 1.98 Å long.

Table 3. Association Constants K_a and Free Binding Enthalpies $\Delta G = -RT \ln K_a$ for 1:1 Complexes between Symmetrical Trications and 8 Determined by NMR Titrations in Methanol-d_4 or D_2O at 20 °C

tication[a]	K_a [M^{-1}] in CD_3OD	$-\Delta G$ [kcal/mol]	K_a [M^{-1}] in D_2O[c]	$-\Delta G$ [kcal/mol]
tris(tetrahydropyrimidine) **10**	$1.8 \times 10^3 \pm 18\%$[b]	4.4		
trisimidazoline **11**	$3.0 \times 10^3 \pm 16\%$[b]	4.7		
tren **18**	$4.8 \times 10^4 \pm 48\%$	6.4	$3.8 \times 10^3 \pm 14\%$	4.9
mesitylene triamine **14** (R = Me)	$8.0 \times 10^4 \pm 34\%$	6.7	$2.6 \times 10^3 \pm 13\%$	4.6
mesitylene triamine **15** (R = H)	$1.4 \times 10^5 \pm 11\%$	7.0	$4.0 \times 10^3 \pm 6\%$	4.9
cyclohexanetriamine **13**	$9.9 \times 10^5 \pm 32\%$	8.1	$1.1 \times 10^3 \pm 15\%$	4.1
trispyrazole **16** (R = Me)	$9.8 \times 10^5 \pm 10\%$	8.0		
trispyrazole **17** (R = H)	$1.0 \times 10^6 \pm 23\%$	8.1		
trisamidine **12**	$1.1 \times 10^6 \pm 8\%$	8.2	$1.0 \times 10^3 \pm 9\%$	4.1

[a] Ammonium and amidinium chlorides (except for **13**, which was used as a bromide). [b] Errors are standard deviations. [c] pD ≅ 7.0.

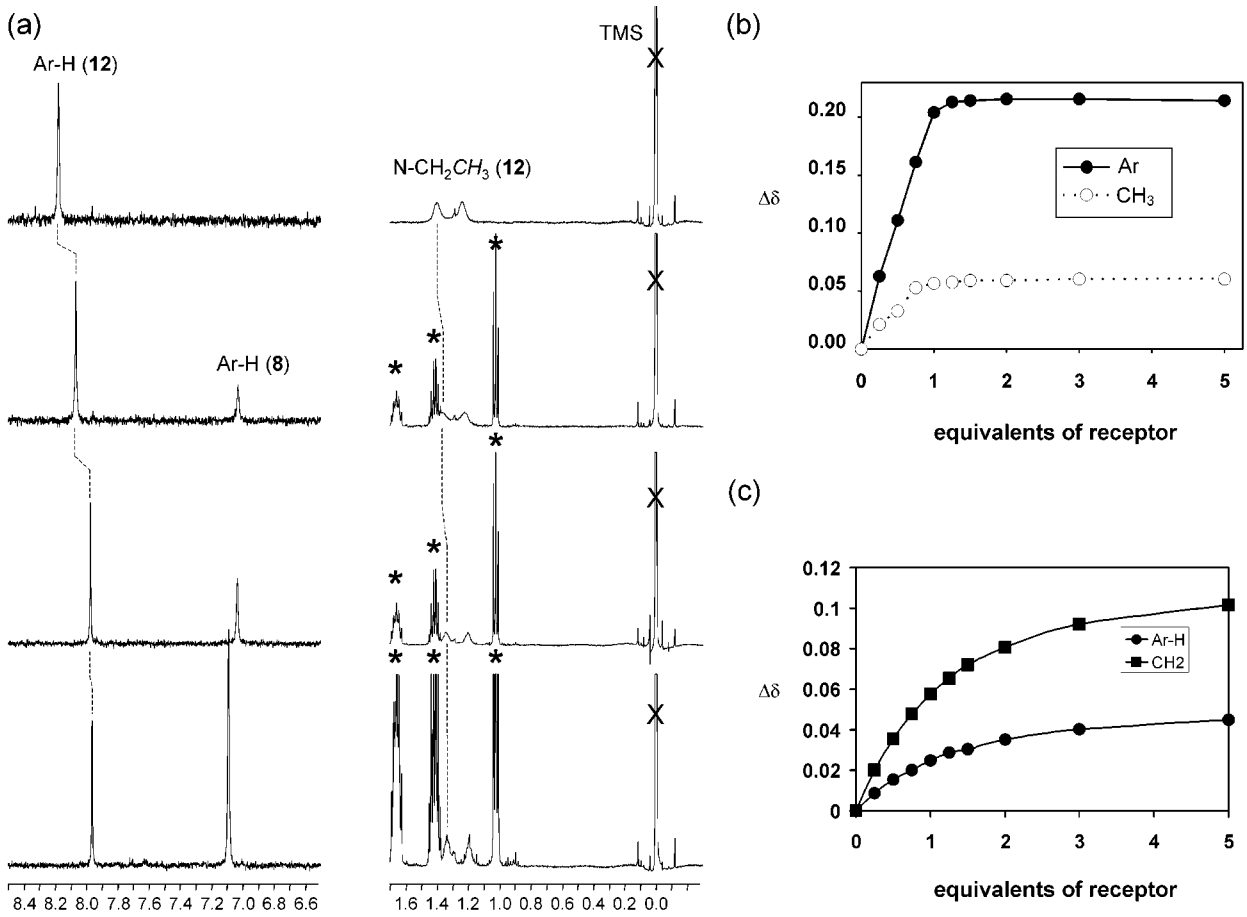

Figure 7. (a) NMR titration of **12** with **8** (from top to bottom: 0, 0.5, 1.0, and 2.0 equiv of **8** added). The two sets of signals for the *N*-ethyl groups indicate that the amidine has a preference for an (*E*,*Z*)-configuration around the C−N partial double bond.[24b] Tetrabutylammonium signals are marked by an asterisk. (b) NMR titration curve showing the change in the chemical shift $\Delta\delta = \delta_{observed} - \delta_0$ for two ^{1}H NMR signals of trisamidine **12** (concn = 0.1 mM) on addition of trisphosphonate **8** in CD_3OD. (c) Typical NMR titration curve for mesitylene triamine **14** with **8** in D_2O.

Obviously, the binding affinity of C_3-symmetrical complementary components for each other is highly dependent on stereoelectronic effects. Whereas the fully conjugated, planar trisimidazoline **10** and the related tris(tetrahydropyrimidine) **11** have to be strongly twisted for complexation by **8** (see above), tris(aminoethyl)amine **18** is much too flexible, and complexation rotations around nine bonds have to be restricted. By contrast, trisamidine **12** and cyclohexanetriamine **13** are more favorably preoriented. The *N*,*N*′-diethyl-substituted amidine **12** with its sterically demanding ethyl groups was found to prefer the (*E*,*Z*)-configuration during complexation with **8** according to ^{1}H NMR spectra of the complex (Figure 7a). In addition, all three amidinium groups of **12** are likely to be strongly twisted relative to the central benzene ring judging from the ^{1}H NMR chemical shift of the aromatic proton ($\delta_H \sim 8.0$) being upfield compared to that of **10** ($\delta_H \sim 8.4$) and **11** ($\delta_H \sim 8.9$). This is in accordance with a previously reported crystal structure in which the torsion angle between a single *N*,*N*′-diethyl-substituted amidinium group and an adjacent phenyl substituent is as high as 66−72°.[24b] Preorganization thus increases the binding constant (Figure 7b,c).

The broad range of association constants that is observed for complexes of **8** with C_3-symmetrical trications therefore reflects the varying degree of preorganization of both complex partners, but there seems to be no obvious correlation with the pK_a values of the protonated triamines/trisamidines.[32] Both components of the complex are flexible molecules possessing various

rotatable bonds that need to be conformationally fixed in the final complex. In this respect, the required entropy loss for the self-organization process lies between that of Rebek's tennisball (composed of rigid half-spheres) and Whitesides' rosette (made up of highly flexible components).[8,33] Several other groups have exploited the multivalency of polytopic ligands, often in a pseudo C_3-symmetrical arrangement.[34] In water, however, solvation effects may become more prominent than the relatively low torsional entropy differences that are in the range of 0.5−3 kcal/mol at 293 K for our aggregates.

We found that most of our complementary trication−trianion complexes are surprisingly stable even in water. Binding constants range from 10^3 to 10^4 M^{-1} for both ammonium and amidinium ligands (Table 3). In aqueous solution, the dominating influence of the electrostatic interaction renders the hard ammonium cation superior to the softer amidinium cation with its delocalized positive charge. Hence, the distribution of association constants becomes much more uniform. Such high binding energies constitute a strong argument for the spheroidal structure of the complexes. In the majority of our C_3-symmetrical arrangements, each ammonium cation is located in the center of two surrounding phosphonate anions, and vice versa. This geometry is favorable considering that the trication and the trianion act as chelates for each other. An alternating order of molecular arms coming from the top and bottom unit generates a compact ball-like structure (Figure 5). Similar combinations of weak multipoint interactions are, of course, also used by Nature for selective and strong self-organization processes.[35]

To gain more insight into the forces governing the self-organization process we carried out microcalorimetric measurements with the aggregate between trisphosphonate **8** and trisamidium salt **12** in water (Microcal MCS−ITC, 20 °C). Aliquots of aqueous **8** were added via microsyringe to a 3 mM aqueous solution of **12**. Strong complexation heats of more than 20 μcal/s were produced even with our small ligands. The titration curve resulted in a K_a value of 400 M^{-1}, a little lower than that of the NMR titration (10^3 M^{-1}). The stoichiometry factor was 0.9, confirming again the 1:1 complex formation. Positive enthalpy and entropy terms were calculated as $\Delta H = +3.5$ kcal/mol and $\Delta S = +12.6$ cal K^{-1} mol^{-1}. This means that, contrary to self-organization processes in unpolar solvents, the enthalpic gain and entropic cost of the interaction between both components are completely overridden by solvation effects. Similar to many other ion-pairing processes in water, the small capsulelike complexes suffer from decreased solvation compared to their highly polar components.[36] In fact, the aggregates are often only poorly soluble in a polar solution. On the other hand, the highly ordered solvation shell around each building block is broken, and free water molecules are released into the solution, leading to entropic gain. In the future, care should be taken to ensure a good solvation of the whole capsule in order to keep the unfavorable positive enthalpy term as low as possible.

We wondered whether the introduction of three ethyl (or methyl) substituents in the 2-, 4-, and 6-positions of trisphosphonate **8** would perhaps increase binding due to preorganization, following an idea that Anslyn and others have previously demonstrated with cationic and neutral receptor molecules.[37] The introduction of three methyl groups in the 2-, 4-, and 6-positions was thought to have the same beneficial effect on triammonium complexation. For practical reasons, we decided to use the more easily accessible trimethyl instead of the triethyl derivatives favored by Anslyn.[18,37b,c,38] This was not without precedence as several groups have used core units of this type and reported crystal structures with an alternating order of substituents in which all the binding sites lie on the same side of the central benzene ring.[39] NMR titrations with various trications and the readily available new "template", 2,4,6-trimethyl-substituted trisphosphonate **9**, proved again that binding in methanol is quite strong and results in the formation of specific 1:1 complexes (Table 4). However, as a direct comparison shows, binding constants are consistently lower than those obtained with the unsubstituted **8** by almost an order of magnitude. We assume that in the lowest energy state, not all phosphonate groups are located on the same side of the central benzene ring of **9**. If this is the case, any phosphonate arm, which has to be rotated to the opposite side of the central benzene ring for three-point binding, experiences an additional steric strain when it passes a neighboring benzylic methyl substituent, thus leading to a reduction in the overall association energy. The same argument applies to the related mesitylene triamines **14** and **15** (Table 3). From the difference in binding energies, a rotational barrier

(32) Potentiometric studies were conducted with an autotitrator and a pH glass electrode with a 3 M KCl internal filling. Titrations were carried out with 0.4905 M NaOH, and about 100 data points were collected for each titration. Protonation constants (pK_a) were obtained by a nonlinear curve fitting of the titration curve or by calculating the pH dependence of the degree of protonation: (a) Billo, E. J. *Excel for Chemists: A Comprehensive Guide*, 2nd ed.; Wiley-VCH: New York, 2001; Chapter 22. (b) Kraft, A. *J. Chem. Educ.*, submitted for publication. In methanol, the different basicities of amines, imidazolines, and amidines are obviously of minor importance. They are much more pronounced in water, and pK_a values could be determined in 0.1 M aqueous KCl at 25 °C for protonated **10** (12.0 ± 0.3, 11.0 ± 0.3, 9.9 ± 0.2), **11** (9.9, 8.7, 7.4), **12** (>11), **13** (10.4, 9.0, 7.2), and **18** (10.3, 9.5, 8.4), in most cases with an error less than ±0.1. The fact that some triamines are not as basic as others and even exist predominantly as diprotonated species at pH 7 (**11**, **13**, **18**) does not seem to affect their association constant with **8** or **9**. We deduce, therefore, that preorientation plays a more important role than the pK_a of the tricationic component.

(33) (a) Seto, C. T.; Whitesides, G. M. *J. Am. Chem. Soc.* **1993**, *115*, 905−916. (b) Seto, C. T.; Whitesides, G. M. *J. Am. Chem. Soc.* **1993**, *115*, 1330−1340.

(34) (a) Prohens, R.; Tomàs, S.; Morey, J.; Deyà, P. M.; Ballester, P.; Costa, A. *Tetrahedron Lett.* **1998**, *39*, 1063−1066. (b) Rao, J.; Lahiri, J.; Weis, R. M.; Whitesides, G. M. *J. Am. Chem. Soc.* **2000**, *122*, 2698−2710.

(35) Mammen, M.; Choi, S.-K.; Whitesides, G. M. *Angew. Chem., Int. Ed.* **1998**, *37*, 2754−2794.

(36) Other groups have found similar ITC results for molecular complexes based on salt bridges in polar solvents: (a) Haj-Zaroubi, M.; Mitzel, N. W.; Schmidtchen, F. P. *Angew. Chem., Int. Ed.* **2002**, *41*, 104−107. (b) Schmidtchen, F. P. *Org. Lett.* **2002**, *4*, 431−434. (c) Linton, B.; Hamilton, A. D. *Tetrahedron* **1999**, *56*, 6027−6038. (d) Sebo, L.; Schweizer, B.; Diederich, F. *Helv. Chim. Acta* **2000**, *83*, 80−92. (e) Enthalpy−entropy compensation often takes place in polar solvents: Dunitz, J. D. *Chem. Biol.* **1995**, *2*, 709−712.

(37) Anion receptors: (a) Ref 18. (b) Metzger, A.; Anslyn, E. V. *Angew. Chem., Int. Ed.* **1998**, *37*, 649−652. (c) Lavigne, J. J.; Anslyn, E. V. *Angew. Chem., Int. Ed.* **1999**, *38*, 3666−3669. Ammonium receptors: (d) Ref 28. (e) Ahn, K. H.; Kim, S.-G.; Jung, J.; Kim, K.-H.; Kim, J.; Chin, J.; Kim, K. *Chem. Lett.* **2000**, 170−171.

(38) As all attempts to chloromethylate 1,3,5-triethylbenzene failed, we chose the commercially available 1,3,5-tris(chloromethyl)-2,4,6-trimethylbenzene instead.

(39) (a) Garratt, P. J.; Ibbett, A. J.; Ladbury, J. E.; O'Brien, R.; Hursthouse, M. B.; Malik, K. M. A. *Tetrahedron* **1998**, *54*, 949−968. (b) Sato, K.; Arai, S.; Yamagishi, T. *Tetrahedron Lett.* **1999**, *40*, 5219−5222. (c) Oh, K. S.; Lee, C.-W.; Choi, H. S.; Lee, S. J.; Kim, K. S. *Org. Lett.* **2000**, *2*, 2679−2681. (d) Yuan, Y.; Zhou, H.; Jiang, Z.; Yan, J.; Xie, R. *Acta Crystallogr., Sect. C* **2000**, *56*, e34−e35.

Table 4. Association Constants K_a and Free Enthalpies $\Delta G = -RT \ln K_a$ for 1:1 Complexes between Symmetrical Trications and 1,3,5-Trimethyl-Substituted Trisphosphonate 9 Determined by NMR Titrations in Methanol-d_4 at 20 °C

tication[a]	K_a [M^{-1}] in CD_3OD	$-\Delta G$ [kcal/mol]	$\Delta\Delta G$[b] [kcal/mol]
tris(tetrahydropyrimidine) **11**	1.2×10^2	2.8	1.6
tren **18**	1.4×10^3	4.3	2.1
trisimidazoline **10**	1.7×10^3	4.3	0.3
mesitylene triamine **14** (R = Me)	3.4×10^4	6.2	0.5
mesitylene triamine **15** (R = H)	5.8×10^4	6.5	0.5
cyclohexanetriamine **13**	1.9×10^5	7.1	1.0
trisamidine **12**	2.1×10^5	7.2	1.0

[a] Ammonium and amidinium chlorides (except for **13**, which was used as a bromide). [b] Difference between ΔG values for trisphosphonates **8** and **9**. These energy differences are attributed mainly to the rotational barrier for one phosphonate moiety as it passes by the neighboring benzylic methyl substituent in **9**.

between 0.3 and 2.1 kcal/mol can be estimated in the above-mentioned series of complexes.[40]

Molecular mechanics calculations of all examined complexes in various environments (gas phase, chloroform, and water) reproducibly led to the same symmetrical complex structures. Detailed conformational searches (Monte Carlo simulations, followed by molecular dynamics calculations) invariably produced global minima with all the flexible arms of each molecule pointing in the same direction, very much like fingers of a claw or like an open mouth. Both complex partners are locked together similar to gear wheels and thus form a molecular capsule. In some of the lower-energy structures, one arm of a half-sphere was opened to the solvent. We assume that opening and closing of arms occurs rapidly and constantly. This, however, distorts only slightly the compact ball-shaped overall structure of the assembly. Calculations of the respective Connolly surfaces[21] revealed a tiny internal cavity. Any attempted inclusion of even small diatomic guests predictably leads to a widening and, thus, destabilization of the capsule; these spheroidal assemblies are considered to be too small for guest encapsulation.[41]

Conclusion

With symmetrical hexacations, it is possible to achieve the spontaneous formation of higher aggregates. Even in water, a 2:1 complex between two half-spheres of **8** and a belt of hexaza-18-crown-6 **19** was formed as we were able to prove by means of a Job plot. The concept for a new design of molecular capsules based on preorientation and alternating charges can thus be transferred to systems with more than two components. Experiments for the directed formation of multicomponent assemblies along these lines are underway in our laboratory. We are also devising larger, more rigid capsules by the same design principles involving cavities large enough to accommodate polar aliphatic and aromatic guest molecules in water. The transport of drugs, sensors, markers, or reagents by such artificial container molecules would, especially in a physiological solution, open the door for a wide range of possible applications.[7]

Experimental Section

General. DMSO-d_6, deuterium oxide, and methanol-d_4 were all purchased in ≥99.8% purity. Thin-layer chromatography (TLC) analyses were performed on silica gel 60 F_{254} with a 0.2 mm layer thickness. Preparative chromatography columns were packed with silica gel 60. All solvents were dried and freshly distilled before use. Compounds **1**,[15] **10**,[23b] **11**,[23c] **12**,[24a] and **13**[25] were prepared according to literature procedures.

1,3,5-Tris(dimethoxyphosphorylmethyl)benzene. 1,3,5-Tris(bromomethyl)benzene[42] (1.00 g, 2.80 mmol) was dissolved in trimethyl phosphite (5 mL) and refluxed for 3 h. Evaporation of the solution gave a colorless oil, which was further purified by column chromatography (9:1 $CHCl_3$/MeOH, $R_f = 0.37$) to furnish a colorless solid. Yield: 1.05 g (84%). Mp: 98 °C. ^{1}H NMR (200 MHz, $CDCl_3$): δ 3.15 (d, $J = 22.1$ Hz, 6 H), 3.68 (d, $J = 10.7$ Hz, 18 H), 7.14 (br q, $J = 2.4$ Hz, 3 H). ^{13}C NMR (75 MHz, $CDCl_3$): δ 32.7 (d, $^1J_{CP} = 138$ Hz), 52.9 (m), 129.9, 132.9. ^{31}P NMR (202 MHz, $CDCl_3$): δ 29.6. MS (CI, NH_3): *m/z* 462 (80%, M + NH_4^+), 445 (25, M + H^+). Anal. Calcd for $C_{15}H_{27}O_9P_3$: C, 40.55; H, 6.13. Found: C, 40.30; H, 6.29.

1,3,5-Tris(dimethoxyphosphorylmethyl)-2,4,6-trimethylbenzene. 1,3,5-Tris(bromomethyl)-2,4,6-trimethylbenzene (1.00 g, 2.51 mmol) was dissolved in trimethyl phosphite (5 mL) and refluxed for 12 h. Evaporation of the solution gave a colorless oil, which was further purified by column chromatography (9:1 $CHCl_3$/MeOH, $R_f = 0.33$). Yield: 0.91 g (74%). ^{1}H NMR (200 MHz, $CDCl_3$): δ 2.44 (s, 9 H), 3.38 (d, $J = 23.5$ Hz, 6 H), 3.64 (d, $J = 10.7$ Hz, 18 H). ^{13}C NMR (75 MHz, $CDCl_3$): δ 18.10, 25.61 (d, $J_{CP} = 130.2$ Hz), 52.50 (d, $J_{CP} = 40$ Hz), 130.58, 138.80. ^{31}P NMR (202 MHz, $CDCl_3$): δ 30.74. MS (CI, NH_3): *m/z* 504 (90%, M + NH_4^+), 487 (35, M + H^+). Anal. Calcd for $C_{18}H_{33}O_9P_3$: C, 44.45; H, 6.84. Found: C, 44.30; H, 6.99.

1,3,5-Tris(hydroxymethoxyphosphorylmethyl)benzene, Tris(tetrabutylammonium) Salt (8). 1,3,5-Tris(dimethoxyphosphorylmethyl)benzene was treated with 3.0 equiv of aqueous [NBu_4]OH and refluxed for 2 weeks. After evaporation of the solvent, the crude product was extracted with chloroform. The solution was dried over $MgSO_4$, filtered, and evaporated to dryness. The colorless amorphous solid was then dried at 50 °C/1 mbar. Yield: 87%. ^{1}H NMR (500 MHz, $CDCl_3$): δ 0.98 (t, $J = 7.6$ Hz, 36 H), 1.41 (sextet, $J = 7.6$ Hz, 24 H), 1.61 (m, 24 H), 2.90 (d, $J = 20.1$ Hz, 6 H), 3.25 (m, 24 H), 3.54 (d, $J = 10.1$ Hz, 9 H), 7.14 (br q, $J = 1.9$ Hz, 3 H). ^{13}C NMR (125 MHz, $CDCl_3$): δ 13.76, 19.72, 24.09, 34.87 (d, $^1J_{CP} = 124.2$ Hz), 51.68 (d, $^2J_{CP} = 5.0$ Hz), 58.30, 128.18, 136.49. ^{31}P NMR (505 MHz, $CDCl_3$): δ 18.58. MS (FAB, glycerol matrix, Xe): *m/z* 1126 (60%, M + H^+), 242 (100, NBu_4^+). Anal. Calcd for $C_{60}H_{126}N_3O_9P_3 \cdot 6H_2O$: C, 58.37; H, 11.27; N, 3.40. Found: C, 58.45; H, 11.51; N, 3.67.

1,3,5-Tris(hydroxymethoxyphosphorylmethyl)-2,4,6-trimethylbenzene, Tris(tetrabutylammonium) Salt (9). 1,3,5-Tris(dimethoxyphosphorylmethyl)-2,4,6-trimethylbenzene was treated with 3.0 equiv of 40% aqueous [NBu_4]OH and refluxed for 3 weeks while the reaction was followed by occasional ^{31}P NMR control. After evaporation of the solvent, the crude product was extracted with chloroform. The solution was dried over $MgSO_4$, filtered, and evaporated to dryness. The colorless amorphous solid was then dried at 50 °C/1 mbar. Yield: 65%. ^{1}H NMR (500 MHz, $CDCl_3$): δ 0.99 (t, $J = 7.3$ Hz, 36 H), 1.43 (sextet, $J = 7.6$ Hz, 24 H), 1.63 (m, 24 H), 2.56 (s, 9 H), 3.13 (d, $J = 20.5$ Hz, 6 H), 3.29 (m, 24 H), 3.57 (d, $J = 10.4$ Hz, 9 H). ^{13}C NMR (125 MHz, $CDCl_3$): δ 13.76, 18.01, 19.72, 24.09, 34.87 (d, $^1J_{CP} = 124.2$ Hz), 51.68 (d, $^2J_{CP} = 5.0$ Hz), 58.30, 128.18, 136.49. ^{31}P NMR (505 MHz, $CDCl_3$): δ 19.88. MS (FAB, glycerol matrix, Xe): *m/z* 1168 (56%, M +

(40) In comparing trisphosphonates **8** and **9**, we assume that the changes in solvation energies on complex formation with their guests are the same for both hosts, since they differ only in three methyl groups on the central phenyl ring.

(41) According to modeling geometries, the egg-shaped inner volume of our capsules was calculated from Connolly surfaces at 0−8 Å^3. Thus, these containers are too tiny even for the smallest conceivable guest, a noble gas atom.

(42) Plater, M. J.; Praveen, M.; Stein, B. K.; Ballantine, J. A. *Tetrahedron Lett.* **1996**, *37*, 7855−7856.

H^+), 242 (100, NBu_4^+). Anal. Calcd for $C_{63}H_{132}N_3O_9P_3$: C, 64.75; H, 11.37; N, 3.60. Found: C, 65.01; H, 11.47; N, 3.78.

General Procedure for the Preparation of 1,3,5-Tris-(phthalimidomethyl)benzene Compounds. The 1,3,5-tris-(bromomethyl)benzene compound, 3.6 equiv of potassium phthalimide, and 0.3 equiv of 18-crown-6 were dissolved in toluene under Ar. After the mixture was heated to 100 °C for 24 h, water was added to the reaction mixture. The aqueous layer was extracted four times with CH_2Cl_2. The combined organic layers were dried over Na_2SO_4 and evaporated, and the residue was purified by column chromatography (20:1 CH_2Cl_2/acetone).

1,3,5-Tris(phthalimidomethyl)benzene. Yield: 71%. R_f = 0.55 (20:1 CH_2Cl_2/acetone). ^{1}H NMR (500 MHz, CD_2Cl_2/$CDCl_3$): δ 4.78 (s, 6 H), 7.35 (s, 3 H), 7.70−7.82 (AA′BB′, 12 H). ^{13}C NMR (125 MHz, CD_2Cl_2/$CDCl_3$): δ 40.23, 122.40, 126.68, 132.16, 133.07, 136.50, 166.95. MS (CI, NH_3): *m*/*z* 573 ($M + NH_4^+$). Anal. Calcd for $C_{33}H_{29}N_3O_6$: C, 71.34; H, 3.81; N, 7.56. Found: C, 71.46; H, 3.70; N, 7.58.

1,3,5-Tris(phthalimidomethyl)-2,4,6-trimethylbenzene. Yield: 82%. R_f = 0.60 (20:1 CH_2Cl_2/acetone). ^{1}H NMR (500 MHz, CD_2Cl_2/$CDCl_3$): δ 2.42 (s, 9 H), 3.57 (s, 6 H), 7.60−7.69 (AA′BB′). ^{13}C NMR (125 MHz, CD_2Cl_2/$CDCl_3$): δ 16.27, 37.54, 122.23, 128.39, 131.01, 132.92, 137.34, 171.03. MS (CI, NH_3): *m*/*z* 615 ($M + NH_4^+$). Anal. Calcd for $C_{36}H_{27}N_3O_6$: C, 72.41; H, 4.56; N, 7.04. Found: C, 72.26; H, 4.45; N, 6.88.

General Procedure for the Preparation of 1,3,5-Tris-(aminomethyl)benzene Compounds. The phthalimide compound was dissolved in a hot mixture of dry EtOH/toluene (2:1) and refluxed with 6 equiv of hydrazine hydrate for 72 h. The reaction mixture was evaporated, and the residue was first suspended in ether and then shaken with a cold 40% aqueous solution of KOH. The extraction was repeated four times, and the combined organic extracts were dried over Na_2SO_4 and filtered. Dry hydrogen chloride was then bubbled through the filtrate. The yellow precipitate was collected by suction filtration and dried.

1,3,5-Tris(aminomethyl)-2,4,6-trimethylbenzene Trihydrochloride (14). Yield: 62%. Mp: 108 °C. ^{1}H NMR (500 MHz, CD_3OD): δ 2.56 (s, 9 H), 4.36 (s, 6 H). ^{13}C NMR (125 MHz, CD_3OD): δ 17.14, 38.90, 131.34, 141.29. MS of the free base (CI, NH_3): *m*/*z* 225 ($M + NH_4^+$). Anal. Calcd for $C_{12}H_{24}Cl_3N_3$: C, 45.74; H, 7.68; N, 13.34. Found: C, 45.46; H, 7.73; N, 13.45.

1,3,5-Tris(aminomethyl)benzene Trihydrochloride (15). Yield: 53%. Mp: 102 °C. ^{1}H NMR (500 MHz, CD_3OD): δ 4.22 (s, 6 H), 7.67 (s, 3 H). ^{13}C NMR (125 MHz, CD_3OD): δ 43.81, 131.73, 136.37. MS of the free base (CI, NH_3): *m*/*z* 183 ($M + NH_4^+$). Anal. Calcd for $C_9H_{18}Cl_3N_3$: C, 39.58; H, 6.64; N, 15.39. Found: C, 39.22; H, 6.45; N, 15.56.

General Procedure for the Preparation of 1,3,5-Tris-(1*N*-pyrazolylmethyl)benzene Compounds. A mixture of the tris(bromomethyl)benzene (1 mmol), 13.2 equiv of pyrazole, four drops of 40% aqueous [NBu_4]OH, and 10 mL of 40% aqueous NaOH in 40 mL of benzene was refluxed for 48 h. The organic layer was separated, dried over Na_2SO_4, and concentrated in vacuo. The residue was dissolved in methanol and treated with 3 equiv of aqueous HCl. After evaporation to dryness, the hydrochloride salt was dried in vacuo.

1,3,5-Tris(1*N*-pyrazolylmethyl)-2,4,6-trimethylbenzene (16). Yield: 86%. ^{1}H NMR (500 MHz, CD_3OD): δ 2.32 (s, 9 H), 5.69 (s, 6 H), 6.61 (m, 3 H), 7.91 (d, J = 2.2 Hz, 3 H), 7.99 (d, J = 2.2 Hz, 3 H). ^{13}C NMR (125 MHz, CD_3OD): δ 17.42, 48.10, 105.90, 129.10, 138.43, 139.40, 140.92. MS of the free base (FAB, glycerol matrix, Xe): *m*/*z* 361 (55%, $M + H^+$). Anal. Calcd for $C_{21}H_{24}N_6$: C, 70.02; H, 6.72; N, 23.33. Found: C, 70.12; H, 6.73; N, 23.45.

1,3,5-Tris(1*N*-pyrazolylmethyl)benzene (17). Yield: 90%. ^{1}H NMR (500 MHz, CD_3OD): δ 5.34 (s, 6 H), 6.36 (t, J = 2.2 Hz, 3 H), 7.58 (m, 3 H), 7.72 (d, J = 2.2 Hz, 3 H), 8.21 (s, 3 H). ^{13}C NMR (125 MHz, CD_3OD): δ 56.16, 105.90, 129.10, 138.43, 140.10, 145.87. MS of the free base (FAB, glycerol matrix, Xe): *m*/*z* 319 (62%, $M + H^+$). Anal. Calcd for $C_{18}H_{21}Cl_3N_6$: C, 50.54; H, 4.95; N, 19.65. Found: C, 50.42; H, 4.73; N, 19.85.

Microcalorimetric Measurements. Microcalorimetric measurements were carried out with the aggregate between trisphosphonate **8** and trisamidium salt **12** in water (20 °C). Aliquots of aqueous **8** were added via microsyringe to a 3 mM aqueous solution of **12**. Complexation heats were more than 20 μcal/s (K_a = 400 M^{-1}; the stoichiometry factor was 0.9; ΔH = +15 kJ/mol, and ΔS = +53 J K^{-1} mol^{-1}). The evaluation software Origin 5.0 was used. The following were the experimental parameters: measuring temperature, 20 °C; room temperature, 17−18 °C; cell volume, 1.414 mL; syringe volume, 250 μL; solvent, triply distilled water; first injection, 5 μL; all other injections, 20 μL; injection period, 60 s; delay time between two injections, 180 s; total number of injections, 11; cell concentration of **12**, 7.34 mg per 2 mL (concn = 3.26 mM); syringe concentration of **8**, 32.8 mg per 1.5 mL (concn = 45.4 mM).

Computational Methods. Molecular mechanics calculations were performed using Cerius^2 software, Molecular Simulations, Inc. The Dreiding 2.21 force field was used. For Monte Carlo simulations and molecular dynamics, the program MacroModel 7.0 was used for model-building procedures and as a graphical interface. Force-field parameters were taken from the built-in force fields, which were in some cases modified versions of the classical published versions. Amber* and OPLAA were chosen for all minimizations and Monte Carlo simulations as well as MD calculations. Both force fields produce essentially the same results. Minimizations were initially carried out in the gas phase and then in aqueous solution. Most complex structures were virtually identical under both conditions, indicating the strong enthalpic preference and hence the stability of these arrangements. Energy minimizations were conducted over 2000 iterations on a Silicon Graphics O2 workstation. The best structures were subjected to conformational searches with 2000-step Monte Carlo simulations. For the optimized conformations, molecular dynamics calculations were subsequently carried out at room temperature for 100 ps and without any external restraints (such as hydrogen bonds, etc.).

^{1}H NMR Titrations. Ten NMR tubes were filled each with 0.80 mL of a solution of the guest compound ($concn_{guest}$ = 0.5−4 mM) in a deuterated solvent (CD_3OD or D_2O). The host compound (1.525 equiv corresponding to the guest) was dissolved in 0.61 mL of the same solvent, and the resulting solution was added, in amounts increasing from 0 to 5.0 equiv, to the 10 guest solutions. Due to their strong hygroscopicity, the tetrabutylammonium phosphonate solutions contained approximately 0.3−0.6% water. Volume and concentration changes were taken into account during analysis. The association constants were calculated by nonlinear regression methods.[14]

Job Plots. Equimolar solutions (10 mmol/10 mL, approximately 10 μM) of trication and trisphosphonate were prepared and mixed in various ratios. ^{1}H NMR spectra of the mixtures were recorded, and the chemical shifts were analyzed by Job's method[13a] modified for NMR results.[13b] Job plots were carried out for complexes of bisphosphonate **1** with dications **2**−**7** as well as for the complexes of trisphosphonate **8** with trications 1,4,7-triazacyclononane trihydrochloride, **11**, **12**, **15**, and **19** and hexacation **19**.

Mass Spectrometric Measurements. Samples (20 μL) for ESI mass spectra were introduced as 10^{-7} M solutions in HPLC-grade methanol at flow rates of 20 μL/min. The heated capillary temperature was 150 °C. The ion spray potential was 3.5 kV (positive ESI), 3.0 kV (negative ESI). About 20−30 scans were averaged to improve the signal-to-noise ratio.

Acknowledgment. We thank Prof. Dr. G. Wulff (Universität Düsseldorf) for generous support during the past three years of T. Grawe's Ph.D. work.

JO025513Y